Concentration Dependence of Loop Fraction in Styrene−Isoprene−Styrene Triblock Copolymer Solutions and Corresponding Changes in Equilibrium Elasticity

Hiroshi Watanabe,* Tomohiro Sato, and Kunihiro Osaki

Institute for Chemical Research, Kyoto University, Uji, Kyoto 611-0011, Japan

Received November 24, 1999; Revised Manuscript Received January 26, 2000

ABSTRACT: Dielectric behavior was examined for solutions of a styrene-isoprene-styrene (SIIS) triblock and SI diblock copolymers in an I-selective solvent, *n*-tetradecane (C14). The SI copolymer had noninverted type-A dipoles in the I block while the SIIS copolymer, a head-to-head coupled dimer of SI, had once-inverted dipoles in the I block. At a low temperature (5 °C) where the S blocks formed glassy, spherical microdomains, the I blocks of SIIS had either the bridge or loop configurations. The loop fraction ϕ_l in these I blocks was estimated from the dielectric losses of the SIIS and SI solutions at low frequencies. The ϕ_l was found to increase (from 0.6 to 0.8) with decreasing SIIS concentration (from 50 to 20 wt %). This increase of ϕ_l was attributed to stretching and destabilization of the bridge configuration on dilution. The equilibrium elasticities of the bridge and dangling loop, estimated from the ϕ_l values and rheological data of the concentrated SIIS/C14 solutions, were comparable in magnitude. This significant elasticity of the dangling loops reflected the strong osmotic constraint on the I block conformation in the concentrated I/C14 matrix phase.

1. Introduction

Styrene−diene−styrene (SDS) triblock copolymers having small S content, typical thermoplastic elastomers, exhibit rubberlike elasticity at low temperatures (T) where the S blocks form glassy, spherical microdomains. This elasticity is related to a network structure of the middle diene blocks that bridge the neighboring S domains.[1] However, a considerable fraction of the middle blocks should be in the loop configuration (having both ends anchored on the same S domain). The contribution of these loops to the elasticity was not clearly understood.

Recently, Watanabe[2] utilized a dielectric method to challenge this loop/bridge problem. *cis*-Polyisoprenes (I) have so-called type-A dipoles[3] parallel along the chain backbone, as found by Adachi and Kotaka.[4] These dipoles enable us to dielectrically observe the global motion of the I chains. For the observation of the I block motion of a SIS copolymer in the rubbery regime (where the I block ends are fixed on the glassy S domain), Watanabe synthesized a SIS copolymer via head-to-head coupling of SI^- anions. This copolymer, having the type-A dipoles inverted at the midpoint of the I block, is hereafter abbreviated as "SIIS" so as to emphasize its dipole-inverted structure. This inversion enabled the dielectric observation of the midpoint motion even in the rubbery regime.

For the SIIS triblock and its precursor SI diblock copolymers, both forming lamellar microdomains in the bulk state, Watanabe found a similar broadening in their slow dielectric mode distributions (detected in a direction essentially parallel to the lamellar normal).[2] This broad mode distribution is attributed to a thermodynamic effect on the I block motion due to the density-preserving requirement.[2,5−7] Arguing a similarity of this effect for the loop- and tail-type I blocks of SIIS and SI and a difference for the bridge- and tail-type I blocks, Watanabe estimated the loop fraction ϕ_l for SIIS from the dielectric loss data of SIIS and SI.[2] The resulting fraction, $\phi_l \cong 0.6$, was in close agreement with theoretical estimates.[8,9]

Those highly populated loops should have significant contributions to rheological properties. Considering this point, Watanabe et al.[10] further examined the equilibrium elasticities of the loop and bridge in a 50 wt % solution of a dipole-inverted SIIS copolymer in an I-selective solvent, *n*-tetradecane (C14). With the above dielectric method, ϕ_l in this solution (containing spherical S domains) was estimated to be ∼0.6. At 15 °C (in the rubbery regime), the elasticities of the loop and bridge evaluated from this ϕ_l were similar in magnitude.[10] This significant elasticity of the dangling loops results from the osmotic constraint on the I block conformation in the concentrated I/C14 matrix phase.

Here, we note that the ϕ_l value in the above concentrated SIIS/C14 solution is close to that in the bulk lamellar system. However, on decrease of the SIIS concentration c, the bridge-type I blocks should be stretched and destabilized. Thus, the bridge fraction ϕ_b ($=1 - \phi_l$) is expected to decrease on dilution. This change in the loop/bridge populations should affect the equilibrium modulus G_e of the SIIS solutions.

From this point of view, we have examined changes in the dielectric behavior of the SIIS/C14 solutions with c. We confirmed the decrease of ϕ_b (increase of ϕ_l) on dilution. Furthermore, we utilized these ϕ_b and ϕ_l data to examine the molecular origin of changes of G_e with c. The results are presented in this article.

2. Experimental Section

The SIIS and its precursor SI samples were synthesized and fully characterized in the previous work.[10] Molecular characteristics of these samples are summarized in Table 1. Dielectric and viscoelastic measurements were conducted at 5 °C for *n*-tetradecane (C14) solutions of SIIS and SI in a range of the copolymer concentration, c/wt % = 20−50. In these solutions, the volume fraction of S blocks was less than 0.12 and the S blocks formed glassy, spherical domains at 5 °C.

* To whom correspondence should be addressed.

10.1021/ma991979f CCC: $19.00
Published on Web 03/10/2000

Table 1. Characteristics of Samples[a]

code	$10^{-3}M$ for block sequence	$10^{-3}M$[b]	M_w/M_n
SI[c]	7.2−17.9	25.1	1.07
SIIS[d]	7.2−17.9−17.9−7.2	50.2	1.07

[a] Cis/trans/vinyl ≅ 75/20/5 for the I block. [b] Total molecular weight. [c] Having noninverted type-A dipoles in the I block. [d] Having symmetrically once-inverted type-A dipoles in the I block.

The SIIS and SI solutions with $c = 20-50$ wt % were prepared by dissolving prescribed amounts of the SIIS/SI sample and C14 in benzene to make homogeneous solutions (with $c \sim 5$ wt %) and then allowing benzene to thoroughly evaporate. (The copolymer concentration was determined from the mass of the residual C14 solution after this evaporation.)

For the SIIS/C14 and SI/C14 solutions, dielectric measurements were carried out at 5 °C in a guarded parallel-plate dielectric cell (of an empty capacitance = 120 pF) with capacitance bridges (GR 1689A, General Radio; HP 4285A, Hewlett-Packard). The equilibrium modulus G_e was determined from creep measurements for the SIIS/C14 solutions and from small amplitude oscillatory tests for the SI/C14 solutions, both at 5 °C with a rheometer (SR-5000, Rheometrics) in a parallel-plate geometry of diameter = 2.5 cm. In the creep measurements, the SIIS solutions exhibited linear responses under small stresses (raising the equilibrium strain <0.02). Similarly, linear responses were observed for the SI solutions at the oscillatory strain amplitudes ≤0.01.

Before the above measurements, the SIIS and SI solutions were annealed at a high temperature (70 °C) where the Newtonian, viscous behavior was observed (i.e., at $T > T_{ODT}$). Then the solutions were slowly cooled to the experimental temperature, 5 °C. With this annealing operation, the dielectric and viscoelastic data were obtained with excellent reproducibility.

3. Results and Discussion

3.1. Overview of Dielectric Behavior. Figure 1 shows the dielectric behavior of the SIIS/C14 and SI/C14 solutions at 5 °C. In respective panels, the behavior is compared for these solutions having the same c. The unfilled and filled circles indicate the dielectric losses ϵ''_{SIIS} and ϵ''_{SI} of the SIIS and SI solutions, respectively. The spherical S domains are in the glassy state at 5 °C, and the dielectric dispersion seen here is exclusively attributed to motion of the I blocks: For SIIS having the once-inverted type-A dipoles in the I block, the dispersion reflects the midpoint motion of the I block having either the bridge or loop configurations.[2,10] For SI having noninverted dipoles, the free end motion of the tail-type I block is observed as the dispersion.[5−7]

The I blocks in the SIIS solutions are barely entangled, as judged from their molecular weight M_{bI} (= 35.8×10^3) and the volume fraction v_{bI} in the I/C14 matrix phase; $M_{bI}/M_e = 0.94$, 1.5, 2.1, and 2.7 for $c =$ 20, 30, 40, and 50 wt %, respectively, where $M_e = M_e°/v_{bI}$ ($M_e° = 5 \times 10^3$ in bulk I systems[11]) is the entanglement molecular weight in the matrix phase. In the SI solutions, the I blocks having smaller M_{bI} (= 17.9×10^3) were even less entangled. For these SIIS and SI solutions, the dispersion shifts to lower ω with increasing c; see Figure 1. This shift, indistinguishable for the SIIS and SI solutions, is primarily attributed to an increase of the local friction in the I/C14 matrix phase with increasing v_{bI}.

In Figure 1, we note that ϵ''_{SIIS} and ϵ''_{SI} depend only weakly on the angular frequency ω and exhibit no terminal tail ($\epsilon'' \propto \omega$) even at the lowest ω examined. Thus, the I blocks of SIIS and SI exhibit significantly broadened dielectric mode distribution, and their terminal relaxation is undetectably slow. This mode distribution, seen as the shape of the ϵ'' curve, is very similar for SIIS and SI at ω below the ϵ''-peak frequency ω_{peak} but is narrower for SI at $\omega > \omega_{peak}$. These similarity and difference of the SIIS and SI solutions provide us with an important clue for dielectrically estimating the loop and bridge fractions, as explained below.

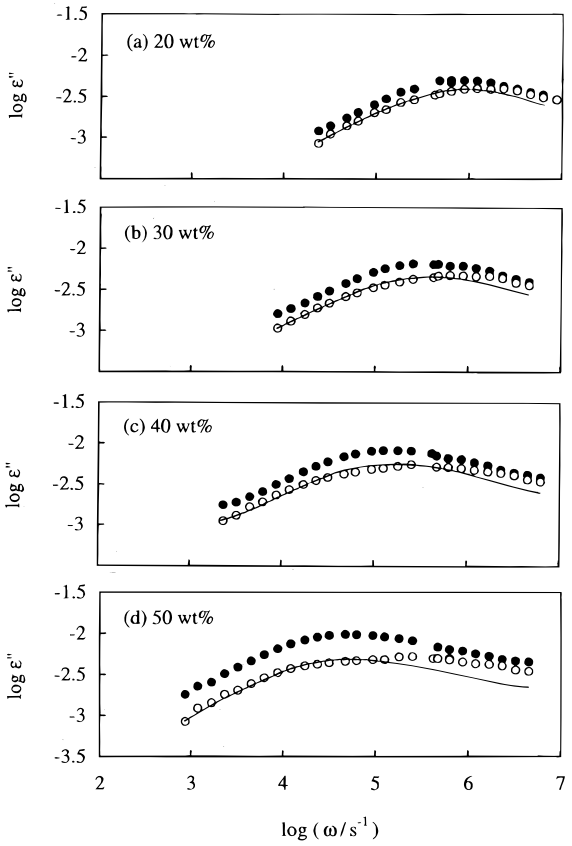

Figure 1. Dielectric behavior of the SIIS/C14 and SI/C14 solutions with the copolymer concentrations as indicated. The ϵ'' data of the SIIS and SI solutions at 5 °C are shown by the unfilled and filled circles, respectively. The solid curves indicate the ϵ''_{SI} data of respective SI solutions multiplied by a factor ϕ_l (loop fraction for SIIS). Note that the SIIS and SI solutions exhibit no terminal behavior ($\epsilon'' \propto \omega$) in the range of ω examined.

3.2. Dielectric Estimation of Loop Fraction. The broad and retarded dielectric relaxation of the tail-type I blocks of SI (Figure 1) is attributed to a thermodynamic (osmotic) constraint on the block conformation:[2,5−7] In the concentrated I/C14 matrix phase, the tails are required to preserve a uniform concentration distribution (to reduce the osmotic free energy), thereby being forced to move in a highly cooperative way. During this cooperative motion, each I block has to take entropically unfavorable, distorted conformations. The corresponding entropic barrier, determined by the end-to-end distance l of the tail, is the origin of the dielectrically observed broadening/retardation of the tail end motion. (The I blocks are prohibited from entering the S domains. However, this spatial confinement for the I blocks has just a secondary effect on the broadening/retardation, as suggested from a statistical calculation for model tails subjected to no osmotic constraint.[12])

Considering a similar osmotic constraint for SIIS, Watanabe et al. made the following argument.[2,10] The loop-type I block of SIIS is composed of two half-

fragments each being identical to the tail-type I block of SI. The two fragments synchronously stretch/retract on the midpoint motion and have nearly the same l to feel nearly the same barrier in almost all cases.[10] In addition, the tension and friction for each fragment are identical to those for the tail. Thus, the two fragments together behave as a hypothetical tail, and the dielectric relaxation functions ψ_l and ψ_t of single loop and tail would satisfy the relationship[2,10]

$$\psi_l(t) = 2\psi_t(t) \tag{1}$$

Here, the factor 2 accounts for a fact that the loop is composed of two half-fragments, each being identical to the tail.

In contrast, for the two half-fragments of the bridge-type I block of SIIS, a change in l of one fragment on the midpoint motion tends to cancel the change for the other fragment. Thus, the net barrier (determined by l's of the two fragments) would be smaller and the dielectric relaxation would be faster for the bridge than for the loop. In addition, under the osmotic constraint, the midpoint may be more localized for the bridge than for the loop (because the two bridge fragments tend to pull the midpoint in the opposite direction), and the dielectric intensity may be smaller for the bridge. These arguments suggest an inequality for ψ_l and ψ_b of the loop and bridge[2,10]

$$\psi_l(t) \gg \psi_b(t) \quad \text{at long } t \tag{2}$$

The dielectric relaxation functions of the SIIS/C14 and SI/C14 solutions are written in terms of the above ψ's as

$$\Phi_{SIIS}(t) = \nu^{(l)}\psi_l(t) + \nu^{(b)}\psi_b(t), \quad \Phi_{SI}(t) = \nu^{(t)}\psi_t(t) \tag{3}$$

Here, $\nu^{(l)}$ and $\nu^{(b)}$ are the number densities of the loop and bridge in the SIIS solution, and $\nu^{(t)}$ is the tail number density in the SI solution.

The dielectric loss ϵ'' is given by the Fourier transformation of $-d\Phi(t)/dt$. For our SIIS and SI solutions having the same c, $\nu^{(l)} + \nu^{(b)} = \nu^{(t)}/2$ ($M_{SIIS} = 2M_{SI}$; cf. Table 1). Thus, eqs 1−3 give a simple relationship for the ϵ''_{SIIS} and ϵ''_{SI} of these SIIS and SI solutions[2,10]

$$\epsilon''_{SIIS}(\omega) \cong \phi_l\epsilon''_{SI}(\omega) \quad \text{at low } \omega \tag{4}$$

Here, $\phi_l = \nu^{(l)}/(\nu^{(l)} + \nu^{(b)}) = 2\nu^{(l)}/\nu^{(t)}$ is the loop fraction in the SIIS solution.

3.3. Concentration Dependence of Loop and Bridge Fractions. Equation 4 suggests that $\epsilon''_{SIIS}(\omega)$ and $\epsilon''_{SI}(\omega)$ exhibit the same ω dependence at low ω *if* the arguments of Watanabe et al.[2,10] are valid. In Figure 1, solid curves show the ϵ''_{SI} data that are multiplied by appropriate factors ϕ_l to achieve the best superposition on the ϵ''_{SIIS} data at low ω. Good agreement of the curves and the unfilled circles (ϵ''_{SIIS}), seen at $\omega < \omega_{peak}$, lends qualitative support to eq 4. Thus, we utilize eq 4 as the working hypothesis to estimate the loop fraction ϕ_l for SIIS (at 5 °C).

In Figure 2, the ϕ_l values estimated by eq 4 are plotted against the SIIS concentration c. (The ϕ_l value for c = 50 wt %, 0.55, agrees well with the previously obtained value[10] at 15 °C.) Clearly, ϕ_l increases with decreasing c. This increase of ϕ_l (the decrease of the bridge fraction ϕ_b) is also noted from the decrease of the difference between the raw ϵ''_{SIIS} and ϵ''_{SI} data (Figure 1).

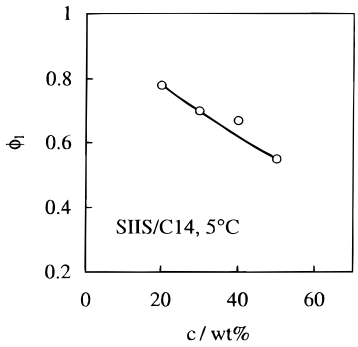

Figure 2. Plots of the loop fraction ϕ_l in the SIIS/C14 solutions against the SIIS concentration.

The above result can be naturally related to the structural change on dilution. In general, the microdomain structures are indistinguishable for A−B/2 diblock copolymers and its dimer-type ABA triblock copolymers.[2,13] In addition, for diblock copolymer micelles in selective solvents, the micellar core radius changes with the copolymer concentration c only moderately; for example, for a styrene-butadiene diblock copolymer ($M = 52 \times 10^3$, S content = 29.5 wt %) in C14, the micellar S core radius r_S increases only by 30% on an increase of c from 11 to 60%.[14]

Thus, in our SIIS/C14 solutions, r_S should have hardly changed and the spacing D between neighboring S domains would have increased (roughly in proportion to $c^{-1/3}$) on the decrease of c from 50 to 20 wt %. For this case, the decrease of c should influence differently the bridge and loop configurations: The bridges (as well as knotted loops) are considerably stretched while the dangling (unknotted) loops are less significantly affected as D increases on dilution. This stretching should increase the conformational free energy of the bridges to reduce their equilibrium population, quite possibly resulting in the observed decrease of ϕ_b on dilution.

3.4. Comments on the Estimated Loop/Bridge Fractions. The arguments of Watanabe et al.[2,10] do not explicitly consider the behavior of knotted (interdigitated) loops/bridges and are applicable to SIIS systems containing only a small number of these knotted chains. Concerning this point, Figure 1 demonstrates interesting changes of ϵ''_{SIIS} with c: The slow dielectric mode distribution of ϵ''_{SIIS}, seen as the shape of the ϵ''_{SIIS} curve at $\omega < \omega_{peak}$, is fairly insensitive to c (in the range between 20 and 50 wt %) and coincides with the slow mode distribution of ϵ''_{SI}. In contrast, the fast mode distribution of ϵ''_{SIIS} (at $\omega > \omega_{peak}$) becomes narrower with decreasing c. Correspondingly, in the entire range of ω, the difference between the ϵ''_{SIIS} and ϵ''_{SI} data becomes smaller on dilution. Specifically, at c = 20 wt %, these data approximately coincide with each other (cf. Figure 1a).

Since the populations of the bridges (in either unknotted and knotted state) and the knotted loops should decrease with decreasing c due to the stretching/destabilization explained earlier, the I blocks in the SIIS/C14 solution would mainly have the dangling loop configuration at small c, e.g., c = 20 wt %. Thus, the approximate coincidence of the ϵ''_{SIIS} and ϵ''_{SI} data at c = 20 wt % strongly suggests that the dangling loops (the major component in the SIIS solution) and tails (in the SI solution) do exhibit very similar dielectric responses. Furthermore, the c-insensitivity of the mode distribution of ϵ''_{SIIS} at $\omega < \omega_{peak}$ suggests that the slow dielectric

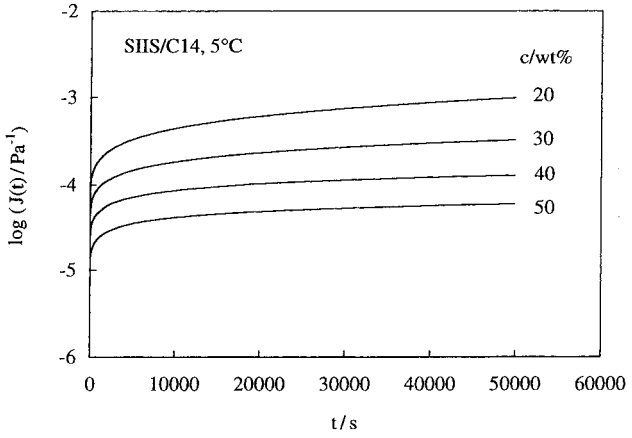

Figure 3. Creep compliance of the SIIS/C14 solutions with the SIIS concentrations as indicated.

relaxation of the SIIS/C14 solution is dominated by the dangling loops in the range of c between 20 and 50 wt %. Thus, the arguments of Watanabe et al. and the resulting relationship (eq 4) seem to be valid for the SIIS solutions examined: In these solutions, the I blocks having $M_{bI}/M_e \leq 2.7$ would not be significantly knotted and obey eq 4.

It should be emphasized that the above validity vanishes for SIIS systems containing heavily knotted I blocks: A statistical calculation for model loops[12] suggested that the tails and heavily knotted loops exhibit different dielectric responses, and eq 4 fails for these chains. Experimentally, a dielectric change attributable to the heavy knot formation was observed on a long-time annealing of a bulk SIIS system at $T > T_g^{PS}$.[15] This result suggested that the heavily knotted loops and bridges cannot be distinguished dielectrically.[15] In fact, this distinction is conceptually unnecessary because various physical properties would be essentially the same for these knotted chains.

In relation to the above dielectric changes on the high-T annealing, we remember that the bulk SIIS system examined by Watanabe[2] was cast from toluene (a common solvent for the S and I blocks) and subjected to the long-time annealing only at $T < T_g^{PS}$. The ϵ''_{SIIS} of this system was proportional to ϵ''_{SI} of the corresponding SI system at low ω, and eq 4 was applicable to the ϵ''_{SIIS} data. The I block configuration in that SIIS system was quite possibly quenched at a barely knotted state at some point during the solvent-casting process.

Concerning the annealing effect, we should also emphasize that the SIIS solutions examined in this study exhibited *no* dielectric change on the annealing at $T > T_{ODT}$ ($> T_g^{PS}$). Thus, at $c = 20-50$ wt %, the relatively short I blocks of SIIS ($M_{bI} = 35.8 \times 10^3$) appear to hardly form heavy knots even after the long-time annealing. This in turn led to the validity of eq 4 for these solutions.

3.5. Concentration Dependence of Equilibrium Modulus. Figure 3 shows the creep compliance $J(t)$ of the SIIS/C14 solutions with the SIIS concentration c as indicated. In Figure 4, the storage moduli G' of the SI/C14 solutions are plotted against the frequency ω.

The G' of the SI/C14 solutions are quite insensitive to ω (<1 s^{-1}). Correspondingly, the loss moduli of these solutions were much smaller than G' (and close to/below the resolution of our experiments). From this elastic response, the equilibrium moduli of the SI solutions were determined as $G_e = [G']_{\omega<1s^{-1}}$.

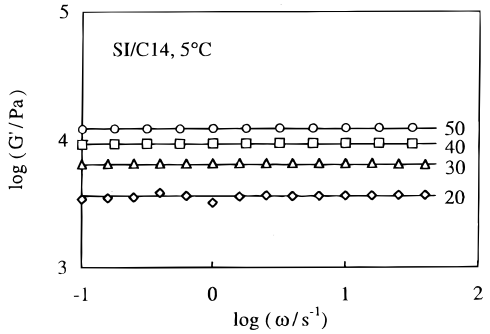

Figure 4. Storage moduli of the SI/C14 solutions. The numbers indicate the SI concentrations (in wt %).

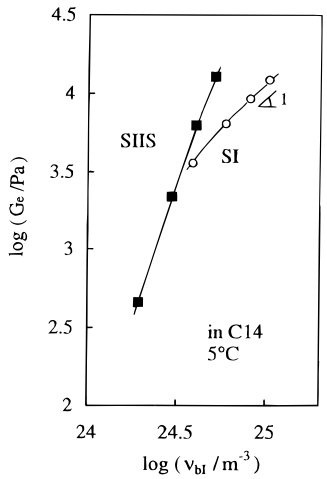

Figure 5. Plots of equilibrium moduli G_e of the SIIS/C14 and SI/C14 solutions (squares and circles) against the number density ν_{bI} of respective I blocks in the solutions. Note that $\nu_{bI}^{SIIS} = \nu_{bI}^{SI}/2$ for the SIIS and SI solutions having the same copolymer concentration.

In contrast, the SIIS/C14 solutions exhibited viscoelastic relaxation with nonnegligible G'' in the range of ω examined (>0.1 s^{-1}). This relaxation, typical of soft rubbers, disturbed the determination of G_e from the G' data. Thus, G_e of the SIIS solutions were evaluated from the $J(t)$ data at long t. The equilibrium plateau of $J(t)$ is almost but not fully attained in the range $t \leq 5 \times 10^4$ s; cf. Figure 3. These $J(t)$ data were fitted with an empirical equation for viscoelastic solids having distribution of retardation times λ_p[10,16]

$$J(t) = \sum_p L_p[1 - \exp(-t/\lambda_p)] \qquad (5)$$

Here, L_p is a discretized retardation spectrum, and the sum $\sum_p L_p$ gives G_e^{-1} of the SIIS solutions.

In Figure 5, the G_e values of the SIIS and SI solutions thus determined are plotted against the number density ν_{bI} of the I blocks in the solutions. For SI, G_e is (almost) proportional to ν_{bI}; see circles. Similar results were found for styrene−butadiene (SB) diblock copolymer micellar solutions in C14 (a B-selective solvent).[7] This proportionality between G_e and ν, observed for well-stabilized micellar lattices of diblock copolymers in selective solvents, indicates that the osmotically constrained micellar corona blocks (tails) are elastically distorted by the applied strain to sustain the equilibrium modulus.[7] (In other words, these corona blocks statically behave as entropic strands under the osmotic constraint on their conformations, despite a fact that they do not bridge the neighboring S domains.)

For the SIIS solutions, G_e depends more strongly on ν_{bI}; see filled squares in Figure 5. This strong ν_{bI} dependence is partly related to changes in the bridge population with c as well as changes in the network structure in the SIIS solutions, as discussed below.

3.6. Loop/Bridge Contributions to Equilibrium Elasticity. The equilibrium modulus of the SIIS/C14 solution is expressed as a sum of contributions from the I blocks having various configurations[10]

$$G_e^{SIIS} = \nu^{(b)} \tilde{G}_e^{(b)} + \nu^{(l,k)} \tilde{G}_e^{(l,k)} + \nu^{(l,d)} \tilde{G}_e^{(l,d)} \quad (6)$$

Here, $\tilde{G}_e^{(b)}$, $\tilde{G}_e^{(l,k)}$, and $\tilde{G}_e^{(l,d)}$ are the modulus per I block having the bridge, knotted (interdigitated) loop, and dangling loop configurations, respectively, and $\nu^{(b)}$, $\nu^{(l,k)}$, and $\nu^{(l,d)}$ are the number densities of respective I blocks. (As explained earlier, the short I blocks in our SIIS solutions appear to hardly form heavy knots. However, for completeness, eq 6 includes the contribution from the knotted loops.)

The total number density of the I blocks of SIIS is given by

$$\nu_{bI}^{SIIS} = \nu^{(b)} + \nu^{(l,k)} + \nu^{(l,d)} \quad (7)$$

In addition, $\nu^{(l,k)}$ and $\nu^{(l,d)}$ can be quantified in terms of the loop fraction ϕ_l (Figure 2) as

$$\nu^{(l,k)} + \nu^{(l,d)} = \phi_l \nu_{bI}^{SIIS} \text{ and } 0 \le \nu^{(l,d)} \le \phi_l \nu_{bI}^{SIIS} \quad (8)$$

In the SI/C14 solutions, the tail-type I blocks entropically sustain the static stress because of the strong osmotic constraint on their conformations. This stress-generating mechanism is similar for those tails and the dangling loops in the SIIS solutions.[10] Thus, $\tilde{G}_e^{(l,d)}$ of the dangling loop in a given SIIS solution can be estimated from the G_e^{SI} data of the corresponding SI solution having the same c[10]

$$\tilde{G}_e^{(l,d)} = \tilde{G}_e^{(t)} = G_e^{SI}/\nu^{(t)} \quad (9)$$

Here, $\tilde{G}_e^{(t)}$ is the equilibrium modulus per tail-type I block in the SI solution, and $\nu^{(t)}$ ($=\nu_{bI}^{SI}$) is the number density of the tails. (Entanglements for the tails and dangling loops, if any, fully relax for sufficiently long time scales and have no contribution to $\tilde{G}_e^{(t)}$ and $\tilde{G}_e^{(l,d)}$. In fact, G_e^{SI} is essentially proportional to ν_{bI}^{SI} (circles in Figure 5), not to $[\nu_{bI}^{SI}]^2$ ($\sim c^2$) as expected for the entanglement plateau modulus.)

The contribution $\tilde{G}_e^{(l,k)}$ of the knotted loop to the equilibrium modulus cannot be accurately quantified. However, this contribution should be between those of the bridge and dangling loop and specified by an inequality

$$\min[\tilde{G}_e^{(l,d)}, \tilde{G}_e^{(b)}] \le \tilde{G}_e^{(l,k)} \le \max[\tilde{G}_e^{(l,d)}, \tilde{G}_e^{(b)}] \quad (10)$$

Applying eqs 6−10 to the G_e^{SIIS} and G_e^{SI} data (Figure 5), ϕ_l data (Figure 2), and the known ν_{bI}^{SIIS} and ν_{bI}^{SI} values, we can specify a possible range of the bridge elasticity $\tilde{G}_e^{(b)}$ in respective SIIS solutions. Table 2 summarizes the $\tilde{G}_e^{(b)}$ thus obtained. For comparison, the $\tilde{G}_e^{(t)}$ and $\tilde{G}_e^{(l,d)}$ of the tail and dangling loop are also shown. For $c = 40$ and 50%, $\tilde{G}_e^{(b)}$ is not significantly different from $\tilde{G}_e^{(t)}$ and $\tilde{G}_e^{(l,d)}$. Thus, the contribution of each dangling loop in the SIIS solutions to the equilibrium elasticity is comparable, in magnitude, to the bridge contribution. This result demonstrates that the osmotically constrained loops exhibit significant elasticity even in the dangling state.

Table 2. Equilibrium Moduli $\tilde{G}_e^{(t)}$, $\tilde{G}_e^{(l,d)}$, and $\tilde{G}_e^{(b)}$ per Tail,[a] Dangling Loop,[b] and Bridge[b] in C14 Solutions at 5 °C

c/wt %	$\tilde{G}_e^{(t)}$, $\tilde{G}_e^{(l,d)}/10^{-21}$ Pa m^3	$\tilde{G}_e^{(b)}/10^{-21}$ Pa m^3
20	0.94	0−0.24
30	1.09	0−0.74
40	1.16	1.6−2.4
50	1.19	2.5−4.1

[a] In SI/C14 solutions. [b] In SIIS/C14 solutions.

In a more quantitative aspect, the $\tilde{G}_e^{(b)}$ is a little larger (by a factor 2−3) than $\tilde{G}_e^{(t)}$ and $\tilde{G}_e^{(l,d)}$ at $c = 40$ and 50 wt %. This minor difference may be related to trapped entanglements[1] among bridges and knotted loops in the SIIS solutions. The molecular weight between trapped entanglements is estimated to be $M_e^{trap} = M_e/(\phi_b + \phi_{l,k})$, where ϕ_b and $\phi_{l,k}$ are the fractions of the bridges and knotted loops, respectively, and M_e ($=M_e°/\upsilon_{bI}$) is the entanglement molecular weight defined for all bridges and loops (including the dangling loops) in the I/C14 matrix phase. For the bridges and knotted loops in our SIIS solutions, the trapped entanglement density M_{bI}/M_e^{trap} estimated from ϕ_b ($=1 - \phi_l$) and $\phi_{l,k}$ (between 0 and ϕ_l) are $M_{bI}/M_e^{trap} = 1.4 \pm 0.7$ and 2 ± 0.7 for $c = 40$ and 50 wt %. Thus, the entanglements may have been just lightly trapped in these solutions to raise the above small difference between $\tilde{G}_e^{(b)}$ and $\tilde{G}_e^{(t)}$.

Table 2 also indicates that $\tilde{G}_e^{(b)}$ is smaller than $\tilde{G}_e^{(t)}$ and $\tilde{G}_e^{(l,d)}$ at $c = 20$ and 30 wt %. In particular, at $c = 20$ wt %, the difference between $\tilde{G}_e^{(b)}$ and $\tilde{G}_e^{(t)}$ is unequivocally concluded from a ratio of the raw moduli data, $G_e^{SIIS}/G_e^{SI} = 0.13$ (cf. Figure 5); this ratio is significantly smaller than the ratio of the block number densities, $\nu_{bI}^{SIIS}/\nu_{bI}^{SI} = 0.5$. Thus, *on average*, the bridge in the SIIS solutions sustains smaller modulus than the tail in the SI solutions at $c = 20$ and 30 wt %.

The above result may be related to a heterogeneity in the SIIS solutions at small c. The network structure of the bridges (and knotted loops) should be stretched and destabilized on dilution, finally resulting in the syneresis at sufficiently small c. As a presyneresis effect, this structure would become heterogeneous at small c, e.g., $c = 20$ wt %. Qualitatively speaking, the G_e^{SIIS} value is determined by the softest regions in the heterogeneous solution, i.e., the regions where the I block concentration is smaller than the average. Then, an effective number density of the I blocks sustaining the modulus is smaller than the nominal ν_{bI}^{SIIS} calculated from the total copolymer concentration, resulting in an apparent difference between $\tilde{G}_e^{(b)}$ and $\tilde{G}_e^{(t)}$. (In other words, the elasticity of the effectively working bridge in dilute SIIS solutions is expected to be similar, in magnitude, to that of the tail.)

4. Concluding Remarks

In the microphase-separated solution of the dipole-inverted SIIS triblock copolymer in an I-selective solvent, *n*-tetradecane, the I blocks have either the bridge

or loop configurations. We have dielectrically estimated the loop and bridge fractions ϕ_l and ϕ_b in the SIIS solution at low T (where the spherical S domains were glassy and the solution exhibited rubberlike elasticity). The ϕ_b decreased (ϕ_l increased) with decreasing copolymer concentration c_{SIIS}. The decrease of ϕ_b is attributed to an increase in a distance D between neighboring S domains on dilution: The bridge is stretched/destabilized and its equilibrium population decreases on the increase of D.

The equilibrium modulus G_e of the SIIS solution decreases with decreasing c_{SIIS} in accordance to the above changes of ϕ_l and ϕ_b. Analyses on the basis of the ϕ_l and ϕ_b data suggested that the contributions of individual loops and bridges to G_e are essentially the same in magnitude. This result demonstrates an importance of the *osmotic constraint* on the I block conformation: Because of this constraint, the loops sustain the equilibrium elasticity even in the dangling state.

Acknowledgment. T.S. gratefully acknowledges support from a JSPS Research Fellowship for Young Scientist.

References and Notes

(1) See, for example: *Thermoplastic Elastomers—A Comprehensive Review*; Legge, T., Holden, N. R., Schroeder, H. E., Eds; Hanser Publishers: Munich, Germany, 1988.
(2) Watanabe, H. *Macromolecules* **1995**, *28*, 5006.
(3) Stockmayer, W. H. *Pure Appl. Chem.* **1967**, *15*, 539.
(4) Adachi, K.; Kotaka, T. *Macromolecules* **1984**, *17*, 120.
(5) Yao, M.-L.; Watanabe, H.; Adachi, K.; Kotaka, T. *Macromolecules* **1991**, *24*, 2955.
(6) Yao, M.-L.; Watanabe, H.; Adachi, K.; Kotaka, T. *Macromolecules* **1991**, *24*, 6175.
(7) Watanabe, H. *Acta Polym.* **1997**, *48*, 215.
(8) Zhulina, E. B.; Halperin, A. *Macromolecules* **1992**, *25*, 5730.
(9) Matsen, M. W.; Schick, M. *Macromolecules* **1994**, *27*, 187.
(10) Watanabe, H.; Sato, T.; Osaki, K.; Yao, M.-L.; Yamagishi, A. *Macromolecules* **1997**, *30*, 5877.
(11) Graessley, W. W. *Adv. Polym. Sci.* **1974**, *16*, 1.
(12) Watanabe, H.; Sato, T.; Osaki, K.; Matsumiya, Y.; Anastasiadis, S. H. *Nihon Reoroji Gakkaishi* (*J. Soc. Rheol. Jpn*) **1999**, *27*, 173.
(13) Hashimoto, T.; Shibayama, M.; Kawai, H. *Macromolecules* **1980**, *13*, 1237.
(14) Shibayama, M.; Hashimoto, T.; Kawai, H. *Macromolecules* **1983**, *16*, 16.
(15) Karatasos, K.; Anastasiadis, S. H.; Pakula, T.; Watanabe, H. *Macromolecules* **2000**, *33*, 523.
(16) Ferry, J. D. *Viscoelastic Properties of Polymers*, 3rd ed.; Wiley: New York, 1980.

MA991979F